ARTICLES
PUBLISHED ONLINE: 17 NOVEMBER 2014 | DOI: 10.1038/NPHOTON.2014.280
nature photonics

Photon number resolution enables quantum receiver for realistic coherent optical communications

F. E. Becerra[1]*, J. Fan[2] and A. Migdall[2]

Quantum-enhanced measurements can provide information about the properties of a physical system with sensitivities beyond what is fundamentally possible with conventional technologies. However, this advantage can be achieved only if quantum measurement technologies are robust against losses and real-world imperfections, and can operate in regimes compatible with existing systems. Here, we demonstrate a quantum receiver for coherent communication, the performance of which not only surpasses the standard quantum limit, but does so for input powers extending to high mean photon numbers. This receiver uses adaptive measurements and photon number resolution to achieve high sensitivity and robustness against imperfections, and ultimately shows the greatest advantage over the standard quantum limit ever achieved by any quantum receiver at power levels compatible with state-of-the-art optical communication systems. Our demonstration shows that quantum measurements can provide real and practical advantages over conventional technologies for optical communications.

Measurements based on the quantum properties of physical systems have revolutionized our understanding of information and have enabled many tasks that are not possible by any classical means. Measurements taking advantage of quantum resources have given birth to quantum communication[1,2] and quantum metrology[3,4], which are crucial for many quantum technologies, including quantum computing[5,6], with potential capabilities far beyond the limits of their classical counterparts. Quantum measurements for the discrimination of non-orthogonal coherent states, which cannot be perfectly discriminated due to their inherent quantum noise[7], can enable discrimination below the standard quantum limit (SQL)[8–10] and approach the ultimate limit allowed by quantum mechanics. These measurements have great potential for improving communication technologies and many quantum information applications.

Coherent states are excellent carriers of quantum and classical information due to their intrinsic resilience to loss and their high-spectral-efficiency capabilities. Optical communications based on coherent states can now reach terabit-per-second transmission rates[11,12]. However, the growing need for even higher data transmission rates for communications, cloud computing and other virtualization applications[13] has motivated extensive research into novel multilevel modulation and multiplexing communication formats[14,15], and low-noise signal amplification[16,17] and processing[18] protocols to further improve spectral efficiency and overall information exchange fidelity. State-of-the-art optical coherent receivers for non-orthogonal coherent states employ direct coherent homodyne or heterodyne detection and are now approaching their ultimate sensitivity limit[19,20], the SQL. However, quantum mechanics allows for a much lower error bound for non-orthogonal state discrimination—the Helstrom bound[7]. For example, the SQL is about 10^6 times higher than the error rate given by the Helstrom bound for discriminating coherent states in the quadrature phase shift keying (QPSK) format for a mean photon number of 10. Measurements below the SQL and approaching the Helstrom bound have an unprecedented potential for improving the spectral efficiency and sensitivity of communication systems and also final communication fidelities. However, this potential can only be accessed by employing quantum receivers performing beyond the SQL. Dolinar found an optimal feedback discrimination strategy[21] that can discriminate two non-orthogonal coherent states with error probabilities at the Helstrom limit. Bondurant generalized the Dolinar receiver for QPSK states[22] and found two near-optimal strategies that surpass the SQL for QPSK, which, in the limit of high input powers, have error probabilities with the same exponential scaling as the Helstrom limit. In recent theoretical work, Izumi *et al.*[23] and Nair *et al.*[24] have studied discrimination strategies implementing adaptive measurements that also have the same exponential scaling of the error probability as the Helstrom limit for QPSK in the high-input-power limit and that can be generalized to larger numbers of input states[24]. However, there is no known optimal strategy for reaching the Helstrom limit for QPSK. Recent work has demonstrated a quantum receiver that can unconditionally discriminate two states marginally below the SQL in the single-photon regime[9] and, more recently, a quantum receiver for four QPSK states achieved performance below the SQL for mean photon numbers up to 15 with an unconditional advantage of 6 dB over the SQL[10]. However, even implementations of receivers that only surpass the SQL after correcting for receiver inefficiencies[25–28] have not demonstrated this more modest performance across the range of input powers from a few photons to power levels compatible with current optical communications systems. This raises the question of the real advantage and applicability of quantum receivers for optical communications.

Here, we demonstrate a quantum receiver, using photon number-resolving (PNR) detection, that discriminates multiple coherent states below the SQL with mean photon numbers ranging from a few photons to many photons (20 or higher),

[1]Center for Quantum Information and Control, MSC07-4220, University of New Mexico, Albuquerque, New Mexico 87131-0001, USA, [2]Joint Quantum Institute, University of Maryland, and National Institute of Standards and Technology, 100 Bureau Drive, Gaithersburg, Maryland 20899, USA.
*e-mail: fbecerra@unm.edu

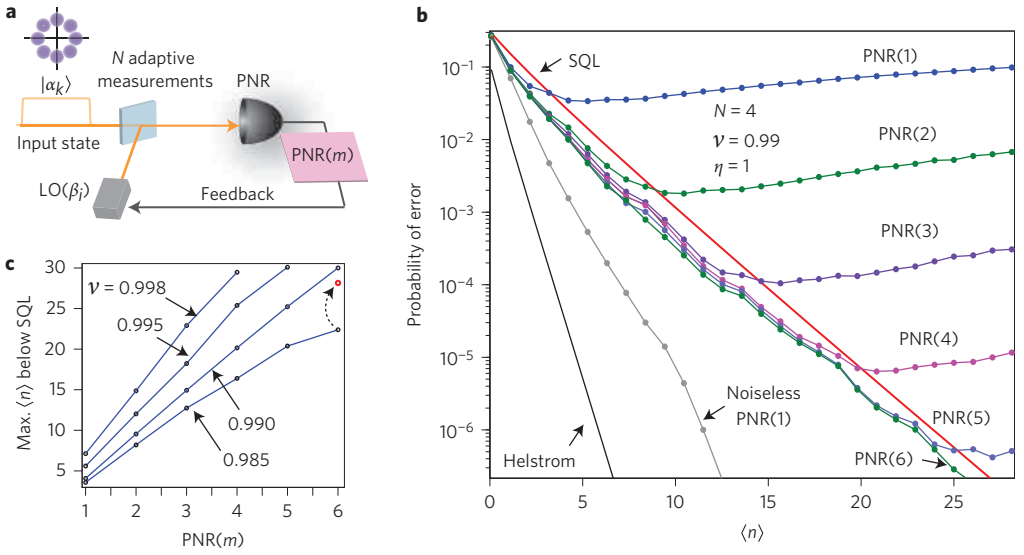

Figure 1 | Robust receiver with photon number resolution. a, Schematic of receiver. The quantum receiver implements N adaptive measurements based on displacement operations and PNR detection to discriminate an input coherent state $|\alpha_k\rangle$ with error probabilities below the SQL. **b**, Probability of error for the discrimination of four non-orthogonal states in the QPSK format as a function of the mean photon number $\langle n \rangle$ for receivers implementing $N = 4$ adaptive measurements with detection efficiency $\eta = 1$ and different PNR powers (from PNR(1) to PNR(6)) in the presence of noise and imperfections resulting in a visibility of $\mathcal{V} = 99\%$. The case of noiseless PNR(1) with $\mathcal{V} = 100\%$, the SQL and the Helstrom bound are also shown for reference. **c**, Maximum mean photon number that can be reached with error probabilities below the SQL for quantum receivers with $\eta = 1$ and $N = 4$ and with different PNR powers for several levels of noise and imperfections resulting in different $\mathcal{V}$. The one red point shows the improvement achieved for a receiver with PNR(6) by increasing the adaptive measurements from $N = 4$ to $N = 5$ with $\mathcal{V} = 98.5\%$, as indicated by the dashed arrow.

making it compatible with both quantum information technologies and state-of-the-art coherent communications. This receiver, implemented with moderate photon number resolution, discriminates QPSK states with a mean photon number of 20 with error probabilities 14.5 dB below the ideal SQL, and our experimental observations point towards even lower error probabilities for higher mean photon numbers. Our receiver is based on adaptive measurements. It shares principles with previously proposed[22,29] and demonstrated[10] receivers, although with PNR detection providing high sensitivity and robustness against imperfections. It is similar to the receivers proposed in refs 30 and 31, which assume idealized PNR detection with infinite resolution. However, our demonstrated receiver is instead based on realistic PNR detection with finite photon number resolution, which is a key feature for making practical use of the receiver in a real communication system. Although PNR detection has been used for the preparation[32] and characterization of quantum states[33] and detectors[34], as well as for quantum-enhanced measurements[35–38], we show specifically that moderate photon number resolution provides robustness for state discrimination. Our demonstrated receiver achieves the greatest advantage over the SQL ever observed by any quantum receiver in the regime with many photons, providing a way to bridge quantum-enhanced measurements for state discrimination from few-photon to high-power levels, and to take advantage of the vast potential of these measurements for optical communications. As a concrete example, we show the advantages of using our photon number resolution-based receiver for coded communications with high spectral efficiency in comparison with conventional SQL-limited receivers.

PNR robust quantum receiver

Figure 1a shows a quantum receiver implementing N adaptive measurements based on optical displacement operations $\hat{D}(\beta)$ of input state $|\alpha_k\rangle$ using a local oscillator reference field (LO) and PNR detections, similar to refs 30 and 31 but with realistic photon number-resolving powers PNR(m). Here, $m-1$ corresponds to the maximum photon number that can be identified by the PNR detector (that is, the possible outputs from the detector are 0, 1, 2, …, $m-1$, and $\geq m$), as opposed to an idealized PNR detector with infinite number resolution. PNR detection provides more information about noise and receiver imperfections in realistic situations than non-PNR detection, and is what allows our quantum receiver to optimize its performance under realistic conditions.

The most significant imperfections preventing the receiver from achieving its optimal performance are the mismatches between the input field and the LO in amplitude, polarization, frequency and spatial and temporal modes, as well as phase noise[39]. To some extent, the effects of these imperfections can be quantified by the interference visibility between the input and the LO fields. The imperfect visibility has limited the performance of demonstrated quantum receivers, particularly at high input powers[9,10,25], because the effects of reduced visibility on the receiver's performance scale with the mean photon number of the input state. Photon number resolution can help to overcome this limitation by providing more information about the reduction in visibility. Accordingly, a quantum receiver based on adaptive measurements, which can enable discrimination approaching the Helstrom bound[10,25,29], and with PNR capability, is expected to extend its range of sub-SQL performance to high input powers[30,31] and beyond what quantum receivers have previously achieved.

In each adaptive measurement i ($i = 1, 2, \ldots, N$), the receiver applies a displacement $\hat{D}(\beta_i)$ to the input state $|\alpha_k\rangle$ in an M-ary PSK format, where $\alpha_k = |\alpha_k|\exp(i\phi_k)$ and $\phi_k = \frac{2\pi k}{M}$ ($k = 1, 2, \ldots, M$), followed by PNR detection with PNR power PNR(m), which is ideally described by the measurement operators $\{\hat{\Pi}_0, \hat{\Pi}_1, \hat{\Pi}_2, \ldots, \hat{\Pi}_{m-1}, \hat{\Pi}_m\}$, with $\hat{\Pi}_j = |j\rangle\langle j|$ for j-photon detection, and $j < m$ and $\hat{\Pi}_m = I - \sum_{l=0}^{m-1} \hat{\Pi}_l$. The probability of detecting d_i photons in period i is given by $\mathbb{P}(d_i|\beta_i, \alpha_k) = \langle\alpha_k|\hat{D}^{\dagger}(-\beta_i)\hat{\Pi}_{d_i}\hat{D}(-\beta_i)|\alpha_k\rangle = (\langle n\rangle_i^{d_i}/d_i!)\exp(-\langle n\rangle_i)$ where $\langle n\rangle_i = \frac{1}{N}(|\alpha|^2 + |\beta|^2 - 2\mathcal{V}|\alpha||\beta|\cos\{\arg(\alpha_k) - \arg(\beta_i)\})$ is the mean photon number of the displaced field in period i and $\mathcal{V}$ is the interference visibility, which quantifies the imperfections of the receiver. The reduction

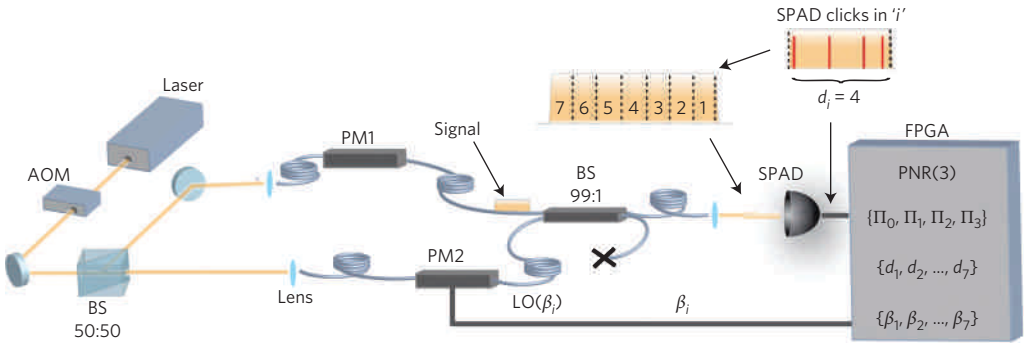

Figure 2 | Experimental implementation of a receiver. The receiver discriminates among four possible QPSK states, prepared by phase modulator PM1, by performing seven adaptive measurements based on optical displacement of the input state in a 99:1 beamsplitter (BS) (combiner) with the local oscillator field LO(β_i) and PNR detection with PNR(3). During each adaptive measurement period i, the single-photon avalanche diode (SPAD) detects d_i photons and the field-programmable gate array (FPGA) uses the total number of detected photons to optimize subsequent adaptive measurements implemented by controlling the phase of the LO using PM2 based on the strategy with a maximum photon number resolution of 3, PNR(3). That is, while in each period i the SPAD can detect many photons, in our implementation any detection $d_i \geq 3$ is counted as three photon detections. The implementation of higher PNR powers is not limited by our SPAD (because its deadtime and recovery times are 8×10^{-3} times smaller than the period duration), but only by the memory of the FPGA, for real-time data processing. Using an FPGA with larger memory and bandwidth for real-time data processing and feedback would allow the implementation of receivers with higher PNR powers. An acousto-optic modulator (AOM) is used to prepare flat-top light pulses of 37 μs from a HeNe laser source.

in system detection efficiency η due to losses and detector inefficiency coherently rescales the input state $|\alpha\rangle$ to $|\sqrt{\eta}\alpha\rangle$, while dark and background counts simply increase $\langle n\rangle$ by $n_{\rm dark}$. The receiver uses the information acquired in each adaptive measurement to optimize subsequent measurements based on a recursive Bayesian strategy[29]. In each period i, the receiver tests a hypothesis β_i with the same amplitude and phase as the most probable state $|\alpha_{\max\{P\}}\rangle$ chosen from the set of possible input states $\{|\alpha_k\rangle\}$ based on the histories of detections $\{d_1, d_2, \ldots, d_N\}$ and displacements $\{\beta_1, \beta_2, \ldots, \beta_N\}$ using the recursive rule[29]:

$$\boldsymbol{P}_{\rm post}(\{|\alpha_k\rangle\}|\beta_i, d_i) = \frac{\mathbb{P}(d_i|\beta_i, \{|\alpha_k\rangle\})\ \boldsymbol{P}_{\rm prior}(\{|\alpha_k\rangle\})}{\sum_{\{|\alpha_k\rangle\}} \mathbb{P}(d_i|\beta_i, \{|\alpha_k\rangle\})\ \boldsymbol{P}_{\rm prior}(\{|\alpha_k\rangle\})} \quad (1)$$

where $\boldsymbol{P}_{\rm post}(\{|\alpha_k\rangle\}|\beta_j, d_j)$ and $\boldsymbol{P}_{\rm prior}(\{|\alpha_k\rangle\})$ are the posterior and prior probabilities in period i, respectively, for all possible input states $\{|\alpha_k\rangle\}$, and $\sum_{\{|\alpha_k\rangle\}}$ indicates the sum over all possible states $\{|\alpha_k\rangle\}$. In this way, at each step i, the hypothesis β_i is chosen to exactly null out the most likely state at that point. In each subsequent period, the most probable state $|\alpha_{\max\{P\}}\rangle$ is the one with maximum posterior probability and the Bayesian probabilities are updated so that $\boldsymbol{P}_{\rm post}$ of period i becomes $\boldsymbol{P}_{\rm prior}$ in period $i+1$. Due to this Bayesian updating procedure, the information from all the adaptive measurements previous to period i is contained in the prior probabilities $\boldsymbol{P}_{\rm prior}$ for this period and this information is used for the hypothesis testing and decision process in period i. At the end of period N, the most probable input state determined in period N corresponds to the final decision of the receiver about the input state[29]. The Bayesian probabilities $\boldsymbol{P}_{\rm post}$ and $\boldsymbol{P}_{\rm prior}$ are obtained using photon number resolution, which provides more information about the effects of phase noise and other real-world imperfections as compared to a receiver without PNR detection capability. Using this additional information, the receiver can better optimize its performance in the presence of those imperfections and overcome their effects, becoming more robust and extending the regime of quantum detection beyond what other quantum receivers have achieved.

Figure 1b shows the performance of simulated imperfect receivers with a level of imperfections quantified by $\mathcal{V} = 99\%$, discriminating four non-orthogonal states in the QPSK format implementing $N = 4$ adaptive measurements with perfect efficiency $\eta = 1$. We observe that the performance of receivers detecting only the presence or absence of photons PNR(1), that is, no photon number resolution, is only slightly better than the SQL for a small range of input powers, with the SQL for coherent states in the QPSK format given by

$$P_{\rm SQL} = 1 - \left[1 - \frac{1}{2}\,{\rm erfc}\left(\sqrt{|\alpha|^2/2}\right)\right]^2 \quad (2)$$

where ${\rm erfc}(x) = \frac{2}{\sqrt{\pi}}\int_x^\infty e^{-t^2}\,{\rm d}t$. In contrast, receivers with higher PNR capabilities not only improve the sub-SQL performance, but also significantly extend this performance to higher input powers, demonstrating an enhanced robustness against noise and real-world imperfections. While our previous studies[29] have indicated only marginal improvements through the use of PNR detection for an ideal noiseless and perfect receiver (that is, perfect visibility), this is not the case in the presence of imperfections, as shown in very recent proposals for idealized PNR receivers with infinite photon number resolution[30,31] and under more realistic conditions as seen with our receiver (Fig. 1b). Figure 1c shows the theoretical expected maximum $\langle n\rangle$ at which the quantum receivers with different PNR powers can perform below the SQL for $\eta = 1$ and $N = 4$, and with imperfection levels characterized by different visibilities. These theoretical predictions show that the maximum $\langle n\rangle$ reached below the SQL varies approximately linearly with PNR power m.

Experimental implementation

Figure 2 presents a schematic of the demonstrated receiver. Our experimental implementation takes advantage of the statistical properties of coherent light and uses a single-photon avalanche diode (SPAD) as a PNR detector[40], with maximum resolving power of 3, PNR(3). The input coherent state is a flat-top 37-μs-long coherent pulse, and the receiver implements $N = 7$ adaptive measurements, each with a duration of ~5.2 μs. Active stabilization of the input power, the relative phase difference between the input field and the LO, the temperature of some optical components and the precise polarization adjustment result in an average experimentally determined visibility of $\mathcal{V}_{\rm Exp} = 99.80(5)\%$. All uncertainties quoted in this Article represent one standard deviation, combining statistical and systematic uncertainties. A field-programmable gate array (FPGA) controlled the timing of the experiment (with a repetition rate of 11 kHz), processed the output of the

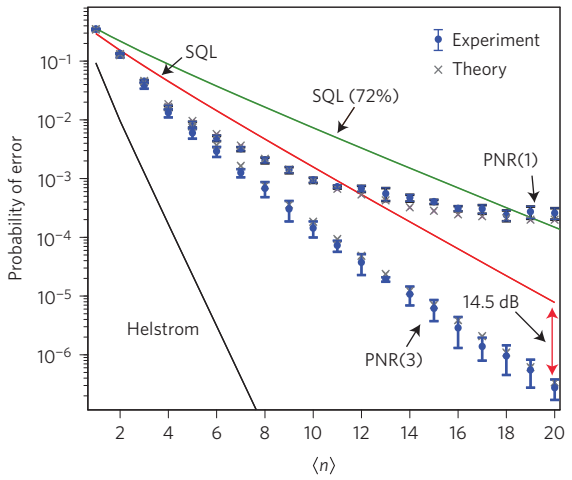

Figure 3 | Experimental results. Error probability (blue symbols) for the discrimination of four non-orthogonal states in the QPSK format by receivers with no PNR power, PNR(1) and with a PNR power of 3, PNR(3). The receiver with PNR(3) can discriminate QPSK states below the SQL for a range that extends to high power levels. It discriminates with much lower errors than its counterpart without PNR capabilities, and reaches error rates 14.5 dB below the ideal, perfect 100% efficiency SQL (red line) and 27 dB below the SQL under the same experimental conditions of detection efficiency (green line). The Helstrom bound is shown for comparison. This receiver reaches error probabilities of 10^{-6} for $\langle n\rangle = 20$ and the data point towards even lower error probabilities at higher $\langle n\rangle$. Error bars represent one statistical standard deviation from four runs of 1×10^6 independent experiments for PNR(1), five runs of 1×10^6 for $\langle n\rangle$ from 1 to 9, five runs of 4×10^6 for $\langle n\rangle$ from 10 to 14 and 10 runs of 4×10^6 for $\langle n\rangle$ from 15 to 20 for PNR(3). The theoretical predictions (crosses) are based on Monte Carlo simulations, with the experimentally determined detection efficiency and visibility for PNR(1) and PNR(3) showing good agreement with the experimental observations.

SPAD in real time, updated the LO for subsequent adaptive measurements based on the strategy with or without PNR detection, and transferred the data to a computer for further analysis. We measured the system detection efficiency to be 72.3(7)%, and a total dark count and background rate of 25 counts per second[29]. We used this receiver for the discrimination of QPSK states with input mean photon numbers $\langle n\rangle$ from 1 to 20 using two different strategies: no photon number resolution (PNR(1)) and with a PNR power of 3 (PNR(3)).

Figure 3 shows the experimental results of the receiver for PNR(1) and PNR(3) together with the Helstrom bound, the ideal SQL and the SQL for a conventional receiver system scaled to the same detection efficiency (72%) as that of our implementation. We observe that the receivers with PNR(1) and PNR(3) both unconditionally surpass the ideal SQL. PNR(1) surpasses this limit for $\langle n\rangle$ from 2 to 11, whereas PNR(3) extends the upper limit to the highest mean photon number we investigated ($\langle n\rangle = 20$), achieving an error probability 14.5 dB below the ideal SQL, and almost a 30 dB improvement over PNR(1). In addition, when compared to the SQL of a system with the same detection efficiency, this receiver surpasses this SQL by a remarkable 27 dB. This receiver reaches error probabilities lower than 10^{-6} and extends the quantum regimes of detection to high mean photon numbers, with the data pointing towards even lower errors at higher $\langle n\rangle$. The theoretical predictions for the performance of our receiver are based on Monte Carlo simulations for a visibility of $\mathcal{V} = 99.8\%$, which is consistent with our measured $\mathcal{V}_{\mathrm{Exp}} = 99.80(5)\%$. We do not observe any significant increase in the error probabilities due to dark and background counts in our numerical studies, as would be expected for receivers with imperfect $\mathcal{V}$. We therefore see that this receiver, which is based only on off-the-shelf components, is robust against noise and realistic imperfections, and can be scaled to higher modulation formats, extending its performance below the SQL to high-input-power levels.

Discussion

Figure 1c shows that the maximum $\langle n\rangle$ achieved with error probability below the SQL is approximately linearly dependent on the PNR power m for small m. Because of the already low error rates achieved by our receiver, the maximum $\langle n\rangle$ that it was practical to investigate experimentally was 20. We used Monte Carlo simulations and the assumption of this linear dependence to infer the expected maximum $\langle n\rangle$ below the SQL achievable by our receiver with $N = 7$ and PNR(3), obtaining a value of 43. We note that state-of-the-art high-sensitivity optical coherent receivers[19,20] discriminate input light pulses with mean photon numbers from about 25 to 70 with error rates ranging from 10^{-4} to 10^{-5}. We estimated the symbol error rate for the demonstrated receiver with PNR(3) at $\langle n\rangle = 43$ to be $\sim10^{-11}$, which is six orders of magnitude smaller than these conventional receivers. We note that, although the sensitivity of non-PNR receivers (that is, PNR(1)) can be raised by increasing the number of adaptive measurements N, this would, however, set stringent limits on the ultimate achievable bandwidth compared to receivers with PNR capabilities. For example, our numerical studies indicate that a non-PNR receiver with detection efficiency of 72% and $\mathcal{V} = 99.8\%$ would require $N = 16$ adaptive measurements to reach error probabilities similar to our demonstrated PNR(3), $N = 7$ receiver for $\langle n\rangle$ from 1 to 20 (Fig. 3). However, this would reduce the reachable bandwidth to 7/16 = 44% of what can be achieved with PNR(3) and $N = 7$, with sub-SQL performance extending to $\langle n\rangle = 29$ versus a maximum $\langle n\rangle = 43$ for our receiver. A PNR(1) receiver with $N = 21$ could achieve sub-SQL performance up to $\langle n\rangle = 40$, but at the expense of a bandwidth three times lower than our receiver. Although our operating pulse rates are much slower than existing systems, we believe that the potential advantages of our quantum receiver will motivate further research aimed at higher rates. We also expect that our demonstration of a robust quantum receiver will motivate research towards incorporating these receivers into long-distance communication links; using an LO field that is independent of the incoming signal field in the receiver's communication node and studying and implementing phase-tracking schemes for these receivers; developing high-speed PNR detectors for achieving rates comparable to homodyne coherent detectors; and integrating these receivers with high-detection-efficiency PNR detectors, allowing for scalability.

We further studied the use of this PNR receiver for coded communications, used in practice to achieve even lower error rates. Specifically, we investigated how the performance of our receiver would improve the implementation of one of the most common coding schemes, the Reed Solomon (RS) codes with parameters (n, k, d), where the codewords have a code length of n symbols with k information symbols and $n–k$ symbols used as redundancies for error correction[41]. Analogous to ref. 26, we calculated the minimum codeword length n_{min} to achieve a desired RS coded error rate $P_{\mathrm{e}}^{\mathrm{RS}}$ as a function of communication code rate $r = k/n$ for different $\langle n\rangle$ for our PNR receiver for QPSK, as described in Fig. 3, and its expected performance with 16 quadrature-amplitude modulation (16QAM) symbols[8]. We calculated the minimum code length n_{min} to achieve a RS coded error rate of $P_{\mathrm{e}}^{\mathrm{RS}} = 10^{-10}$, as described in Supplementary Section I. We selected two input powers to compare the performance of our demonstrated receiver with that of an SQL-limited (heterodyne) 100%-efficient receiver. For completeness, we also included for comparison the performance of an SQL-limited receiver but scaled to the 72% detection efficiency of our receiver.

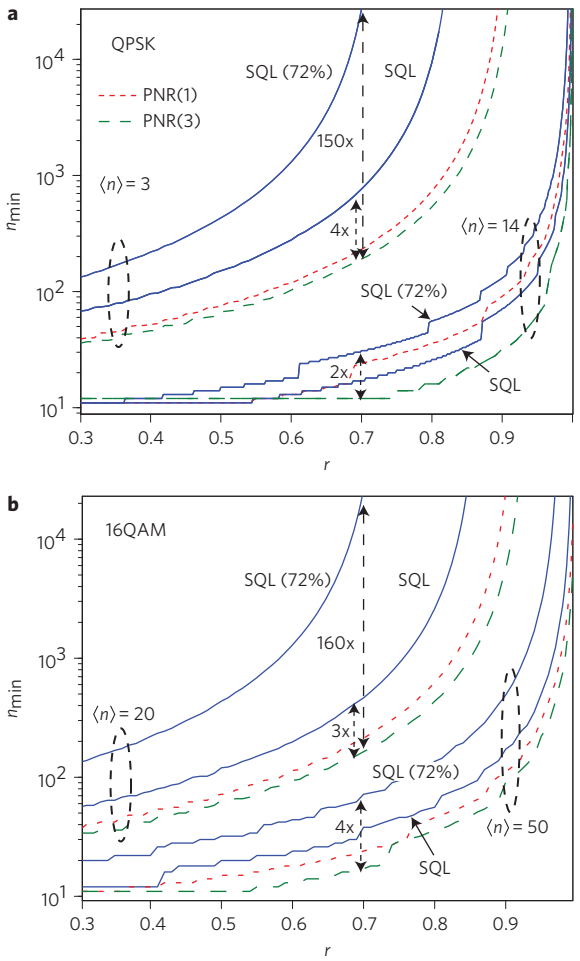

Figure 4 | Minimum codeword length n_{min}. a,**b**, Minimum codeword length n_{min} to achieve an RS coded error probability of $P_e^{RS} = 10^{-10}$ for two sets of input power levels $\langle n \rangle$ for QPSK (**a**) and 16QAM (**b**). The expected performance of the PNR(3) receiver (green dashed lines) is compared with a PNR(1) (red dashed lines) and a conventional SQL-limited receiver (solid blue lines). For completeness, the SQL-limited receiver is also shown scaled to 72% detection efficiency.

As shown in Fig. 4a, for QPSK the n_{min} using our demonstrated PNR(3) receiver is approximately four times smaller than what can be achieved using an ideal SQL-limited receiver and approximately 150 times smaller than with the SQL-limited receiver when correcting for the detection efficiency of our implementation (72%) for $r \geq 0.7$ at small signal powers $\langle n \rangle = 3$. For higher signal powers $\langle n \rangle = 14$, n_{min} is still reduced by a factor of approximately two using our demonstrated PNR receiver, with larger advantages at higher rates r. We also estimated the performance of RS-coded optical communication with 16QAM symbols for high-spectral-efficiency communications[8] for the PNR receiver with $N = 32$, a detection efficiency of 72% and $\mathcal{V} = 99.8\%$. For $\langle n \rangle = 20$, n_{min} was reduced by a factor of approximately three (~160×) when compared to the unscaled (scaled) SQL-limited receiver for $r \geq 0.7$. For higher signal power $\langle n \rangle = 50$, n_{min} was still more than two times (four times) smaller than for the unscaled (scaled) SQL-limited receiver. This simple example demonstrates the potential advantages of our PNR receiver for coded communications with high spectral efficiency under realistic conditions, and one would expect this potential to hold for more sophisticated coding schemes for efficient coded communications. We note that coherent states, with random coding, can achieve the highest possible rate of information that can be reliably transmitted[42] (the Holevo capacity) and the heterodyne measurement is asymptotically optimal in the high-input-power regime. However, a capacity-achieving receiver (measurement) would require the receiver to make joint-detection measurements on long codeword blocks, and its optical implementation is yet to be found. Our receiver can achieve a higher communication rate for information transfer at a desired small codeword error probability for a given code block length as compared to a heterodyne receiver. This could significantly reduce the coding overhead and complexity required to achieve the Holevo capacity as compared to a heterodyne measurement in this high-spectral-efficiency regime.

Robust quantum technologies that can mitigate the effects of realistic imperfections and outperform conventional ones under real-world conditions have great potential for technological advances and for fundamental studies in quantum mechanics. Our demonstrated quantum receiver expands the regimes of non-classical detection to high input power levels for non-orthogonal multi-state discrimination below the SQL, which had previously not been accessible to any demonstrated quantum receiver. Our demonstration complements the study of advanced techniques for high-sensitivity amplification and regeneration of phase-coherent states[16–18] and quantum-enhanced optical phase tracking[43]. Together with advances in fast PNR detectors[44] and fast digital processing, this receiver, implemented in a feed-forward manner allowing for higher rates, could potentially provide a path towards high-spectral-efficiency coherent optical communications below the SQL in amplification-free channels and reduce the need for amplification processes in extended communication links.

Note added in proof: During the preparation of our manuscript, we became aware of related theoretical work by Izumi *et al.*[30] and Li *et al.*[31] studying the improvement of receivers based on detectors with perfect (infinite) photon number resolution, and how these receivers can mitigate the effects of dark counts and mode mismatch in the discrimination process.

Received 26 May 2014; accepted 16 October 2014; published online 17 November 2014

References

1. Gisin, N., Ribordy, G., Tittel, W. & Zbinden, H. Quantum cryptography. *Rev. Mod. Phys.* **74,** 145–195 (2002).
2. Gisin, N. & Thew, R. Quantum communication. *Nature Photon.* **1,** 165–171 (2007).
3. Giovannetti, V., Lloyd, S. & Maccone, L. Advances in quantum metrology. *Nature Photon.* **5,** 222–229 (2013).
4. Abadie, J. *et al.* A gravitational wave observatory operating beyond the quantum shot-noise limit. *Nature Phys.* **7,** 962–965 (2011).
5. Ladd, T. D. *et al.* Quantum computers. *Nature* **464,** 45–53 (2010).
6. Knill, E., Laflamme, R. & Milburn, G. J. A scheme for efficient quantum computation with linear optics. *Nature* **409,** 46–52 (2001).
7. Helstrom, C. W. *Quantum Detection and Estimation Theory, Mathematics in Science and Engineering* Vol. 123 (Academic, 1976).
8. Proakis, J. G. *Digital Communications* 4th edn (McGraw-Hill, 2000).
9. Tsujino, K. *et al.* Quantum receiver beyond the standard quantum limit of coherent optical communication. *Phys. Rev. Lett.* **106,** 250503 (2011).
10. Becerra, F. E. *et al.* Experimental demonstration of a receiver beating the standard quantum limit for multiple nonorthogonal state discrimination. *Nature Photon.* **7,** 147–152 (2013).
11. Jinno, M., Miyamoto, Y. & Hibino, Y. Networks: optical-transport networks in 2015. *Nature Photon.* **1,** 157–159 (2007).
12. Zhou, X. *et al.* 32 Tb/s (320 × 114 Gb/s) PDM-RZ-8QAM transmission over 580 km of SMF-28 ultra-low-loss fiber, in *Proceedings of the National Fiber Optic Engineers Conference (NFOEC)* paper PDPB4 (Optical Society of America, 2009).
13. Armbrust, M. *et al.* A view of cloud computing. *Commun. ACM* **53,** 50–58 (2010).
14. Wang, J. *et al.* Terabit free-space data transmission employing orbital angular momentum multiplexing. *Nature Photon.* **6,** 488–496 (2012).
15. Hillerkuss, D. *et al.* 26 Tbit s^{-1} line-rate super-channel transmission utilizing all-optical fast Fourier transform processing. *Nature Photon.* **5,** 364–371 (2011).
16. Slavik, R. *et al.* All-optical phase and amplitude regenerator for next-generation telecommunications systems. *Nature Photon.* **4,** 690–695 (2010).

17. Tong, Z. *et al.* Towards ultrasensitive optical links enabled by low-noise phase-sensitive amplifiers. *Nature Photon.* **5,** 430–436 (2011).
18. Kakande, J. *et al.* Multilevel quantization of optical phase in a novel coherent parametric mixer architecture. *Nature Photon.* **5,** 748–752 (2011).
19. Tsukamoto, S., Katoh, K. & Kikuchi, K. Unrepeated transmission of 20-Gb/s optical quadrature phase-shift-keying signal over 200-km standard single-mode fiber based on digital processing of homodyne-detected signal for group-velocity dispersion compensation. *IEEE Photon. Technol. Lett.* **18,** 1016–1018 (2006).
20. Kikuchi, K. & Tsukamoto, S. Evaluation of sensitivity of the digital coherent receiver. *J. Lightwave Technol.* **26,** 1817–1822 (2008).
21. Dolinar, S. J. An optimum receiver for the binary coherent state quantum channel. *MIT Res. Lab. Electron. Quart. Progr. Rep.* **111,** 115–120 (1973).
22. Bondurant, R. S. Near-quantum optimum receivers for the phase-quadrature coherent-state channel. *Opt. Lett.* **18,** 1896–1898 (1993).
23. Izumi, S. *et al.* Displacement receiver for phase-shift-keyed coherent states. *Phys. Rev. A* **86,** 042328 (2012).
24. Nair, R., Guha, S. & Tan, S.-H. Realizable receivers for discriminating arbitrary coherent-state waveforms and multi-copy quantum states near the quantum limit. *Phys. Rev. A* **89,** 032318 (2014).
25. Cook, R. L., Martin, P. J. & Geremia, J. M. Optical coherent state discrimination using a closed-loop quantum measurement. *Nature* **446,** 774–777 (2007).
26. Chen, J., Habif, J. L., Dutton, Z., Lazarus, R. & Guha, S. Optical codeword demodulation with error rates below the standard quantum limit using a conditional nulling receiver. *Nature Photon.* **6,** 374–379 (2012).
27. Wittmann, C. *et al.* Demonstration of near-optimal discrimination of optical coherent states. *Phys. Rev. Lett.* **101,** 210501 (2008).
28. Muller, C. *et al.* Quadrature phase shift keying coherent state discrimination via a hybrid receiver. *New J. Phys.* **14,** 083009 (2012).
29. Becerra, F. E. *et al. M*-ary-state phase-shift-keying discrimination below the homodyne limit. *Phys. Rev. A* **84,** 062324 (2011).
30. Izumi, S., Takeoka, M., Ema, K. & Sasaki, M. Quantum receivers with squeezing and photon-number-resolving detectors for *M*-ary coherent state discrimination. *Phys. Rev. A* **87,** 042328 (2013).
31. Li, K., Zuo, Y. & Zhu, B. Suppressing the errors due to mode mismatch for *M*-ary PSK quantum receivers using photon-number-resolving detector. *IEEE Photon. Technol. Lett.* **25,** 2182–2184 (2013).
32. Gerrits, T. *et al.* Generation of optical coherent-state superpositions by number-resolved photon subtraction from the squeezed vacuum. *Phys. Rev. A* **82,** 031802 (2010).
33. Laiho, K., Cassemiro, K. N., Gross, D. & Silberhorn, C. Probing the negative Wigner function of a pulsed single photon point by point. *Phys. Rev. Lett.* **105,** 253603 (2010).
34. Zhang, L. *et al.* Mapping coherence in measurement via full quantum tomography of a hybrid optical detector. *Nature Photon.* **6,** 364–368 (2012).
35. Xiang, G. Y., Higgins, B. L., Berry, D. W., Wiseman, H. M. & Pryde, G. J. Entanglement-enhanced measurement of a completely unknown optical phase. *Nature Photon.* **5,** 43–47 (2011).
36. Afek, I., Ambar, O. & Silberberg, Y. High-NOON states by mixing quantum and classical light. *Science* **328,** 879–881 (2010).
37. Usuga, M. A. *et al.* Noise-powered probabilistic concentration of phase information. *Nature Phys.* **6,** 767–771 (2010).
38. Wittmann, C., Andersen, U. L., Takeoka, M., Sych, D. & Leuchs, G. Demonstration of coherent-state discrimination using a displacement-controlled photon-number-resolving detector. *Phys. Rev. Lett.* **104,** 100505 (2010).
39. Minář, J. c. v., de Riedmatten, H., Simon, C., Zbinden, H. & Gisin, N. Phase-noise measurements in long-fiber interferometers for quantum-repeater applications. *Phys. Rev. A* **77,** 052325 (2008).
40. Banaszek, K., Radzewicz, C., Wódkiewicz, K. & Krasiński, J. S. Direct measurement of the Wigner function by photon counting. *Phys. Rev. A* **60,** 674–677 (1999).
41. Odenwalder, J. P. *Error Control Coding Handbook* (Linkabit, 1976).
42. Giovannetti, V. *et al.* Classical capacity of the lossy bosonic channel: the exact solution. *Phys. Rev. Lett.* **92,** 027902 (2004).
43. Yonezawa, H. *et al.* Quantum-enhanced optical-phase tracking. *Science* **377,** 1514–1517 (2011).
44. Rosenberg, D., Kerman, A. J., Molnar, R. J. & Dauler, E. A. High-speed and high-efficiency superconducting nanowire single photon detector array. *Opt. Express* **21,** 1440–1447 (2013).
45. Polyakov, S. V., Migdall, A. & Nam, S. W. Real-time data-acquisition platform for pulsed measurements. *AIP Conf. Proc.* **1327,** 505–519 (2011).

Acknowledgements

The authors acknowledge financial support from the Physics Frontier Center at the Joint Quantum Institute. F.E.B. thanks J. Kosloski and J. Goldhar for discussions. The authors also thank S.V. Polyakov, who developed the original FPGA-based platform on which our data acquisition system was built[45].

Author contributions

F.E.B. analysed the theoretical measurement strategy, designed the experimental implementation of the receiver, performed the measurements and analysed the experimental results. J.F. realized the analysis for coded communications. J.F. and A.M. provided assistance and discussions. All authors contributed to writing the manuscript.

Additional information

Supplementary information is available in the online version of the paper. Reprints and permissions information is available online at www.nature.com/reprints. Correspondence and requests for materials should be addressed to F.E.B.

Competing financial interests

The authors declare no competing financial interests.